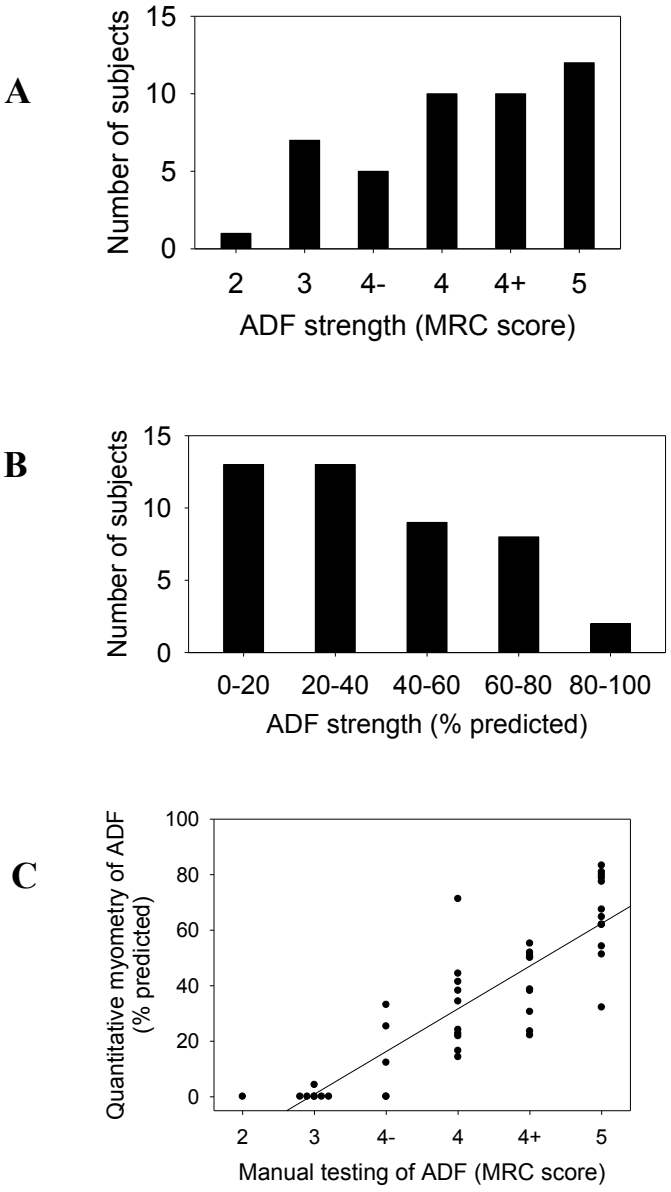

Supplementary Figure 1. Strength of ankle dorsiflexion (ADF) in validation cohort.

Shown are data from 45 subjects with full DM1 mutations. Not shown are 5 subjects with protomutations, all of whom all had grade 5 (normal) ADF strength. Strength was determined on the side that was subsequently used for TA biopsy. A. Distribution of MRC scores by manual testing. B. Distribution of myometry scores by quantitative testing, expressed as the percentage of the predicted strength in a healthy individual of the same age, sex, and height. C. Correlation of manual and quantitative testing ($r = 0.86$, $P < 0.001$).

Pain intensity	0	1	2	3	4	5	6	7	8	9	10
Number of subjects	23	12	12	7	2	1	0	1	0	0	0

Supplementary Figure 2. Tolerability of TA needle biopsy procedure. Report of pain intensity by 58 consecutive DM1 or healthy subjects in the 48 hrs after needle biopsy of TA. Pain was rated on a 10 point scale where "0" indicates no pain and "10" denotes worst pain ever experienced. In separate questions, subjects reported that biopsy experience was "not bad at all" (57%) or "bothered me a little" (43%), whereas none selected "very bothersome" or "horrible". When asked "would you be willing to undergo another needle muscle biopsy", 57 out of 58 subjects answered "yes", and >90% indicated a willingness to consider serial biopsy procedures. All procedures were performed with Bergstrom/University College London side-cut biopsy needles.

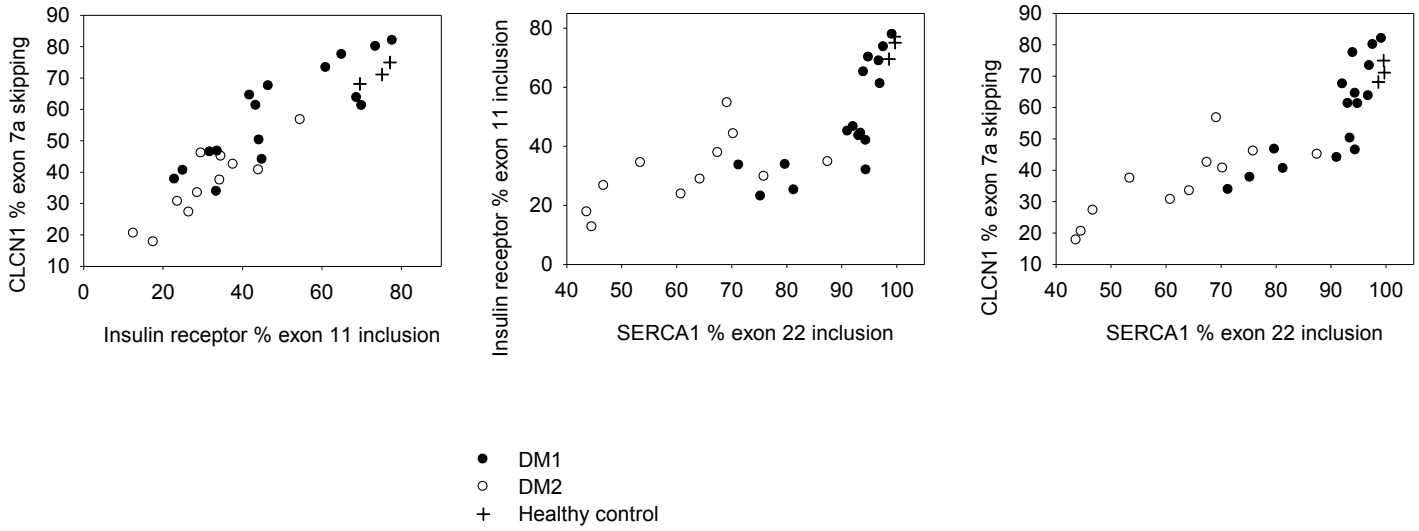

Supplementary Figure 3. Alternative splicing in vastus lateralis muscle in DM1, DM2, and healthy controls. RT-PCR analysis of alternative splicing was performed in VL muscle biopsy samples from 16 individuals with DM1 (filled circles), 11 individuals with DM2 (open circles), and 3 healthy controls ("+" symbols). Three different MBNL1-dependent events were analyzed. For each panel the results are displayed so that increasing severity of splicing misregulation is plotted closer to the origin. Subjects with DM1: 8 females, 8 males, mean age 42 years, range 24 to 71 years; subjects with DM2: 6 male, 5 female, mean age 46 years, range 25 to 69 years; healthy controls: 2 male, 1 female, mean age 42 years, range 25 to 69 years.

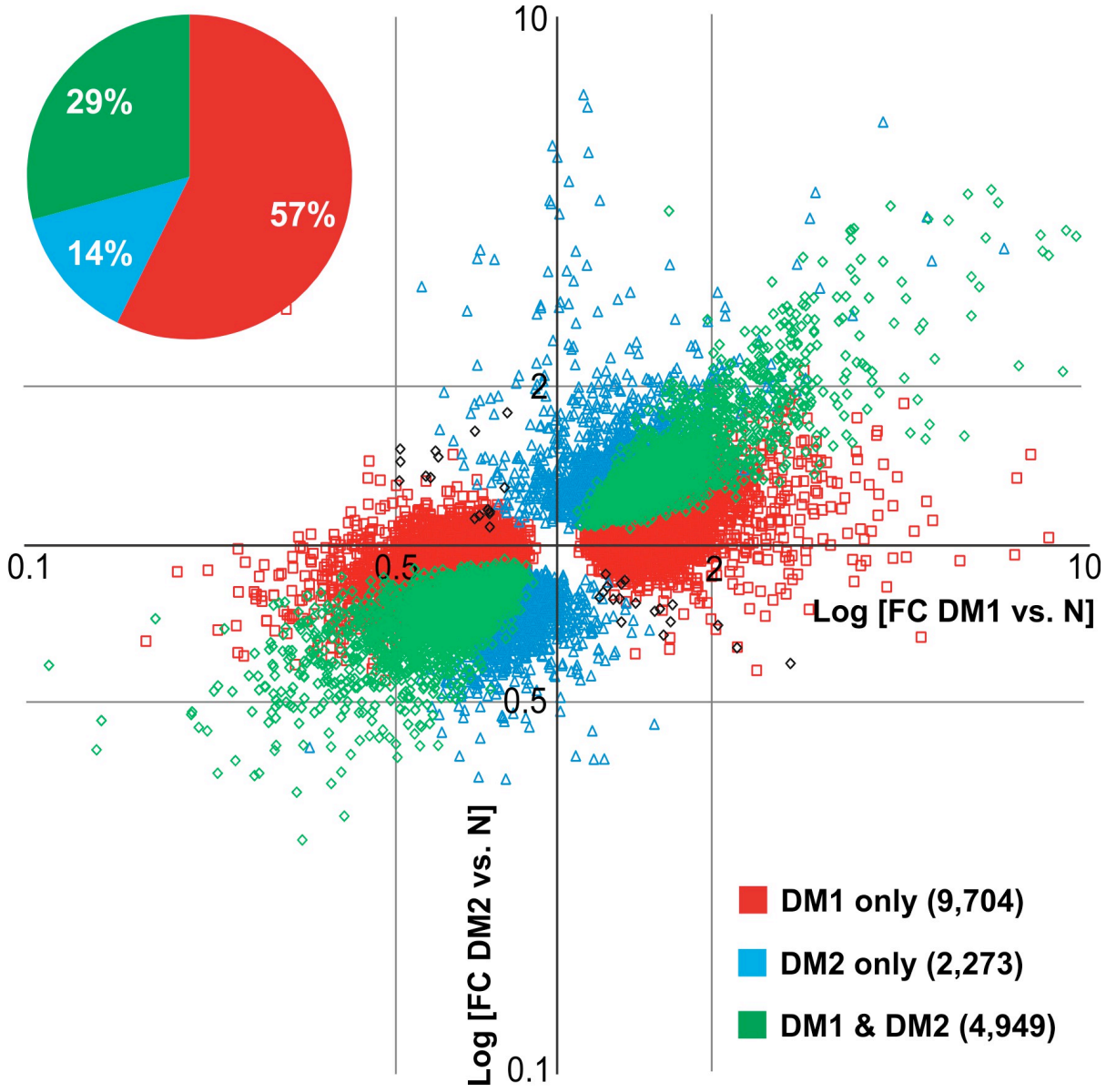

Supplementary Figure 4. Concordance of gene expression changes in DM1 and DM2, based on exon-level data from all-exon arrays. The $\log_2$ fold-change (FC) of probe set (exon) signal intensity is shown for DM1 vs. healthy control (N) on the horizontal axis and for DM2 vs. healthy control on the vertical axis. Core probe sets (exons) showing a trend for differential expression in DM1 vs. normal (nominal $P < 0.01$, red squares), DM2 vs. normal (nominal $P < 0.05$, blue triangles), or both in the same direction (green diamonds) are shown. Out of 16,926

probe sets showing a trend for dysregulation in DM1 or DM2, 4,949 (29%) showed parallel changes in DM1 and DM2, as compared to 35 probe sets that showed changes in the opposite direction (black diamonds). The analysis was performed on 6,600 transcripts and 181,062 core probe sets (exons) that showed clear signal above background (PLIER signal > 200 for the transcript, normalized probe set signal above 50 for the exon, and probe set/transcript signal > 0.05). Probe sets showing a parallel trend for differential expression in FSHD vs. normal (nominal $P < 0.05$), which may reflect non-specific changes of muscle disease, were eliminated from the analysis.

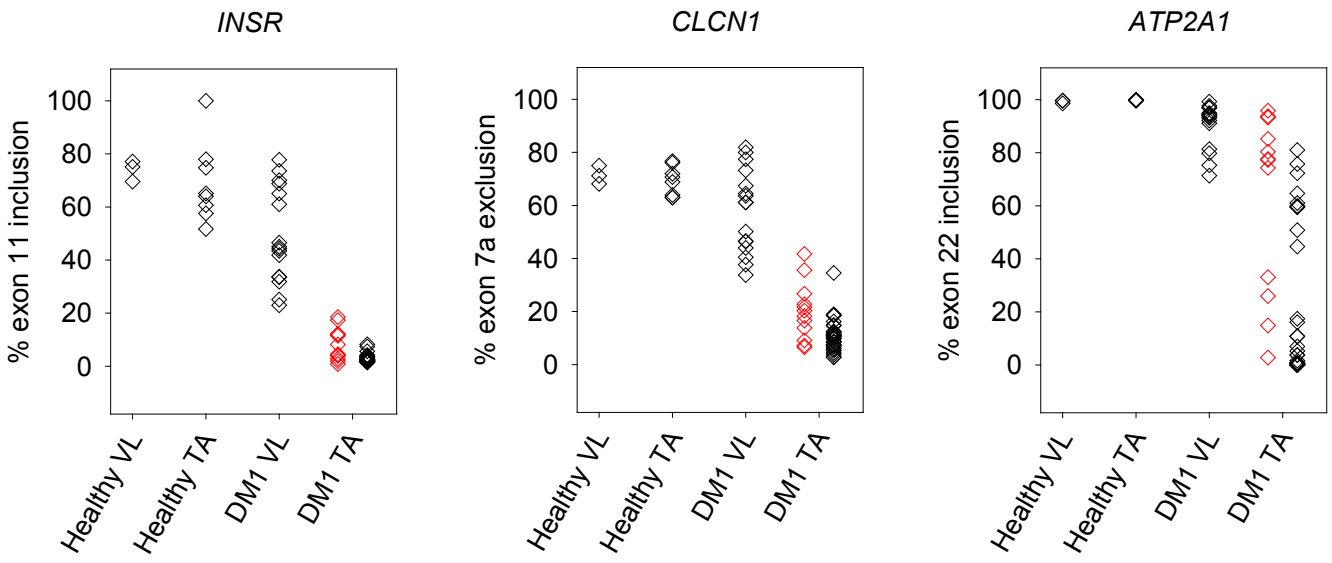

Splice event	Healthy TA	DM1 VL	DM1 TA
ATP2A1 exon 22 inclusion (%)	> 99 ± 0.1	90 ± 9	32 ± 35
INSR exon 11 inclusion (%)	69 ± 15	49 ± 18	4 ± 4
CLCN1 exon 7a exclusion (%)	69 ± 6	58 ± 16	13 ± 9

Supplementary Figure 5. Alternative splicing of insulin receptor (*INSR*), chloride channel 1 (*CLCN1*), and sarcoplasmic reticulum calcium reuptake pump (*SERCA1*/*ATP2A1*) in biopsy samples of vastus lateralis (VL) in the discovery cohort (n = 16) compared to TA samples in the validation cohort (n = 45, protomutation carriers not included). The discovery and validation cohorts were similar in selection criteria (ambulatory adults with full DM1 mutations), age (43 ± 12 vs. 46 ± 11 yrs), and weakness (knee extensors 71 ± 29% vs. 61 ± 22%). For TA muscle samples the results are shown for DM1 subjects with normal ADF strength (MRC grade 5 or 5-, n = 12, red diamonds) and subjects with weakness of grade 4+ or lower (n = 33, black diamonds). Results are also shown for VL from healthy subjects (n = 3) and TA from healthy subjects (n = 8). Alternative splicing was more severely affected by DM1 in TA than VL for each of the three splice events ($P < 10^{-7}$). Summary statistics for splicing data are mean ± SD.

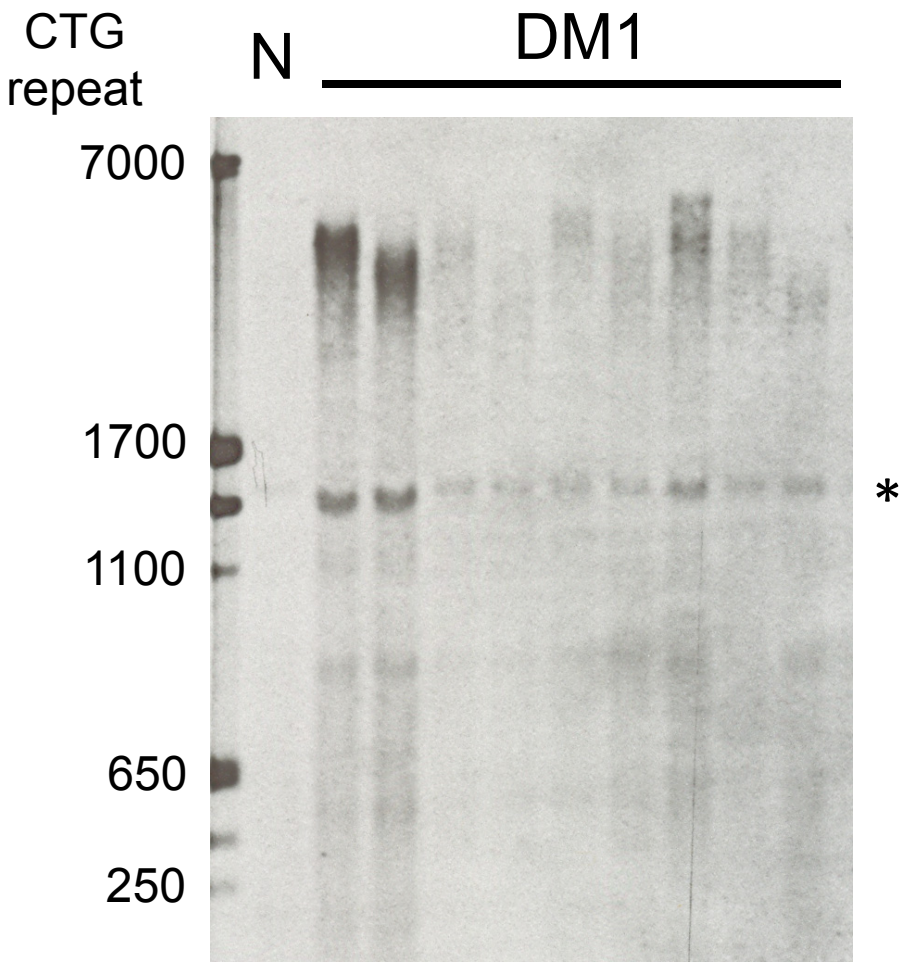

Supplementary Figure 6: Representative Southern blots of expanded CTG repeats in TA muscle tissue. Each lane indicated "DM1" is from a different subject. N, normal control.

* indicates cross-hybridization of probe with genomic fragment that was constant in all subjects.

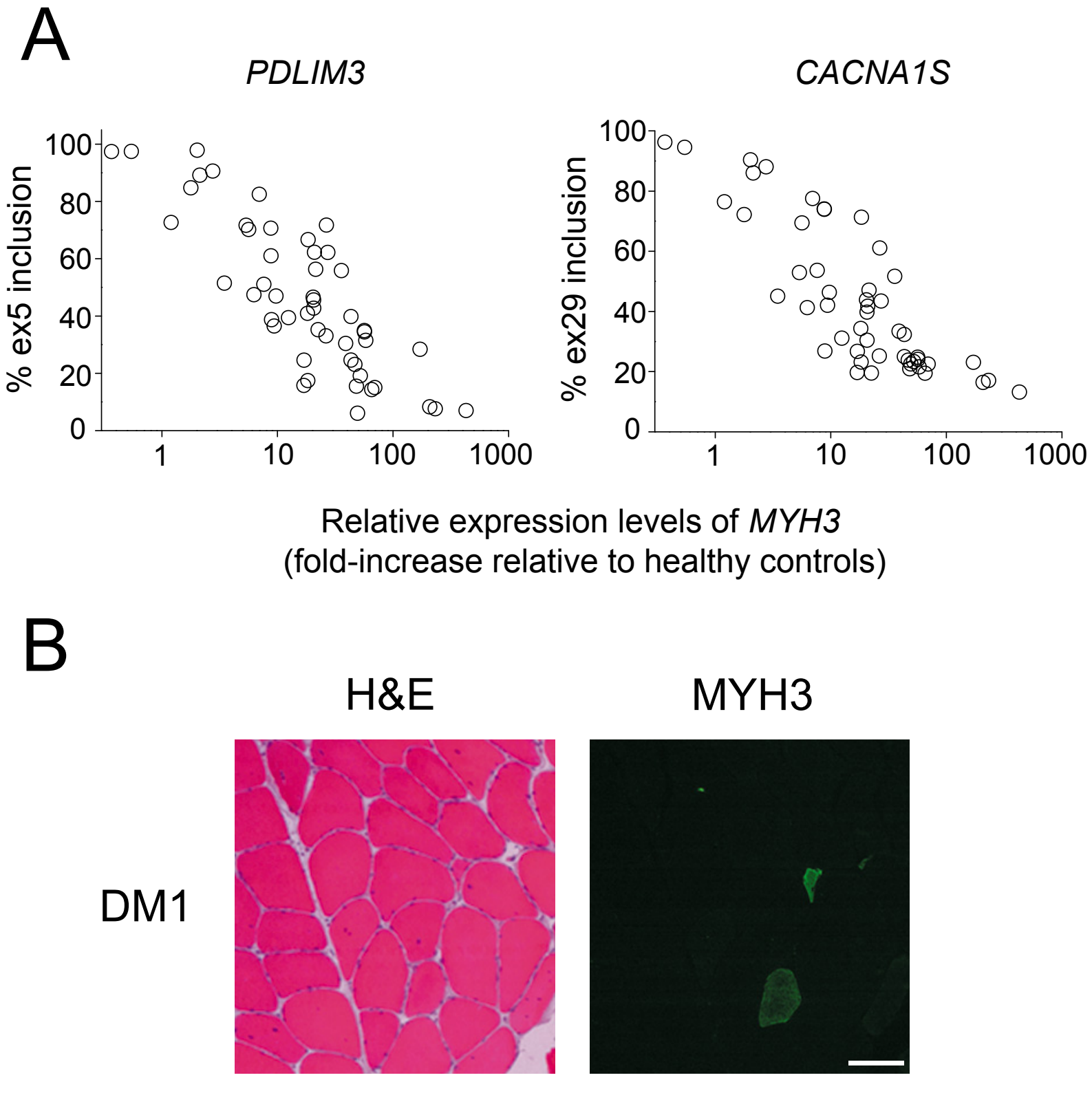

Supplementary Figure 7: Correlation of splicing misregulation with expression of *Embryonic Myosin Heavy Chain* (*MYH3*) mRNA, a molecular marker of muscle regeneration or denervation. **(A)** Two examples of splice events that are correlated with *MYH3* expression, as determined by qRT-PCR: *PDLIM3* encoding a Z disc protein (r = -0.83, $P < 10^{-12}$) and *CACNA1S* encoding the dihydropyridine receptor/voltage gated calcium channel (r = -0.83, $P < 10^{-12}$). *MYH3* mRNA levels are expressed as the fold-change relative to mean value in healthy controls. **(B)** Immunofluorescence of DM1 TA muscle showing that MYH3 protein is expressed in a minor population of muscle fibers. Of note, the MYH3 positive fibers did not show overt changes indicative of muscle regeneration on an adjacent section stained with hematoxylin and eosin (H and E). Bar = 100 μm.

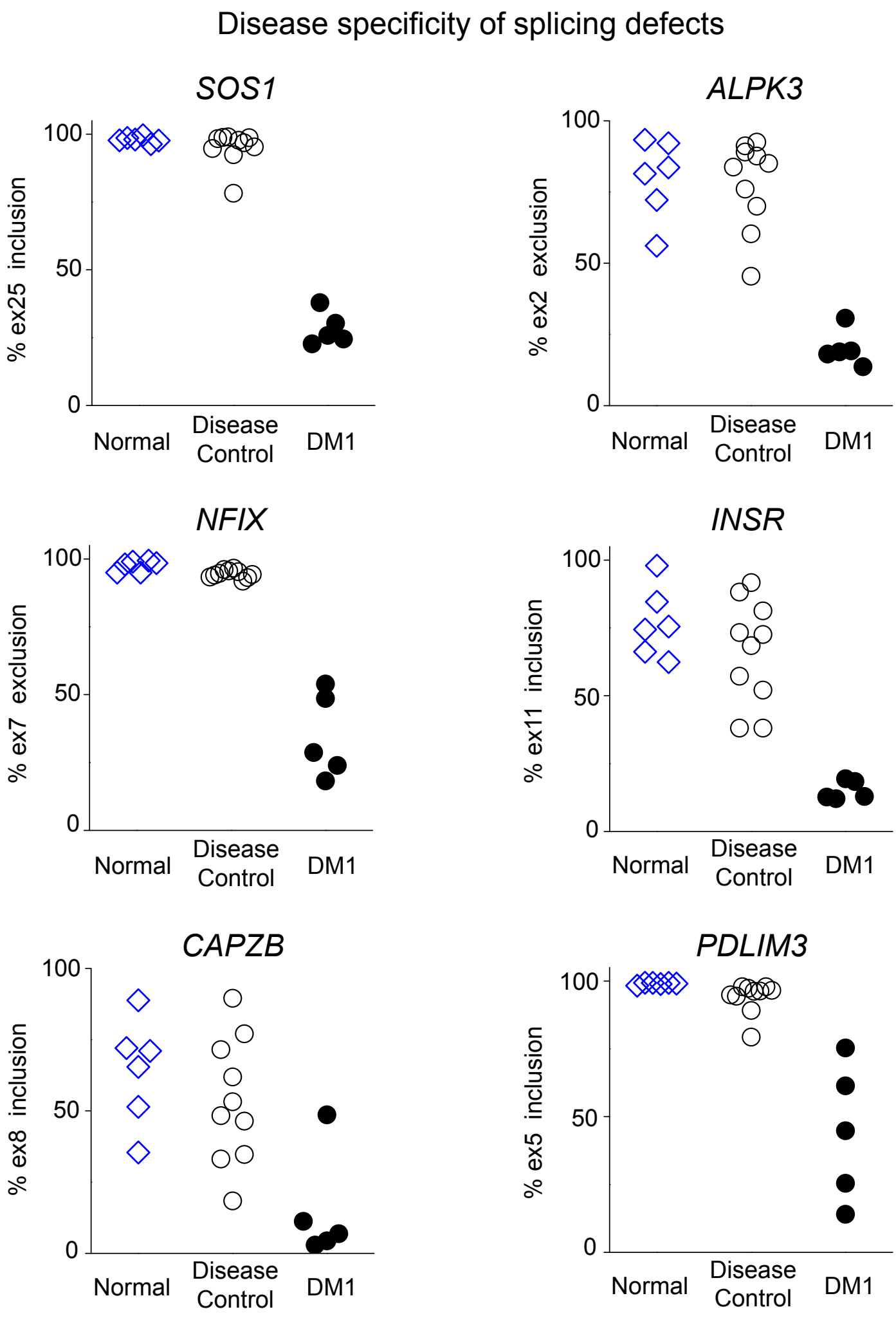
Disease specificity of splicing defects
SOS1
% ex25 inclusion
100
50
0
Normal
Disease Control
DM1
ALPK3
% ex2 exclusion
NFIX
% ex7 exclusion
INSR
% ex11 inclusion
CAPZB
% ex8 inclusion
PDLIM3
% ex5 inclusion

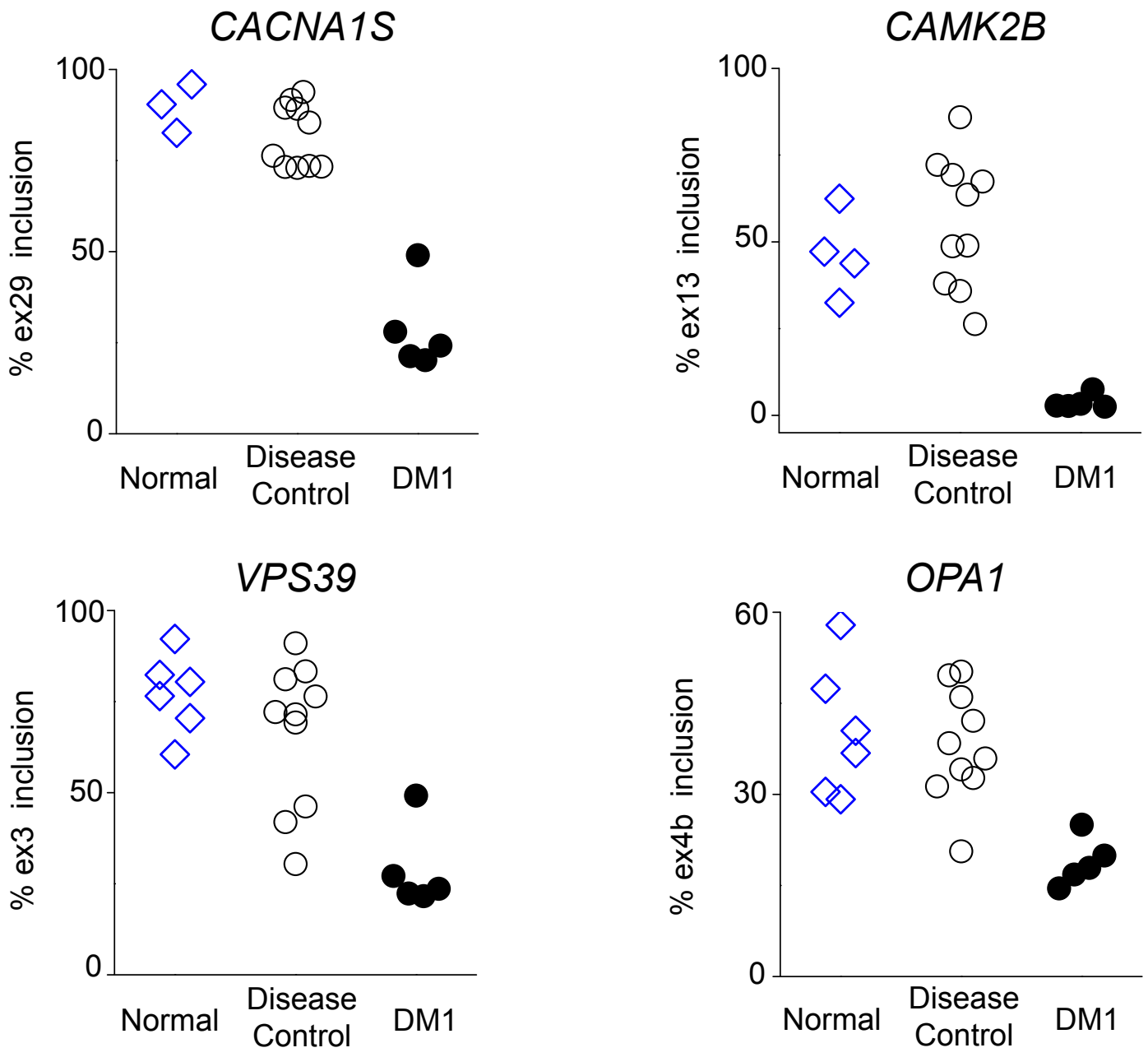

Supplementary Figure 8. Disease specificity of DM-associated splicing defects in TA muscle. Splicing outcome in DM1 (n = 5 or 6 subjects) was compared to healthy controls (n = 3 to 6) and subjects with chronic muscle disease (n = 9 or 10). Disease controls displayed normal or minimally abnormal splicing for the 10 events. Characteristics of disease controls are listed in Supplementary Table 1.

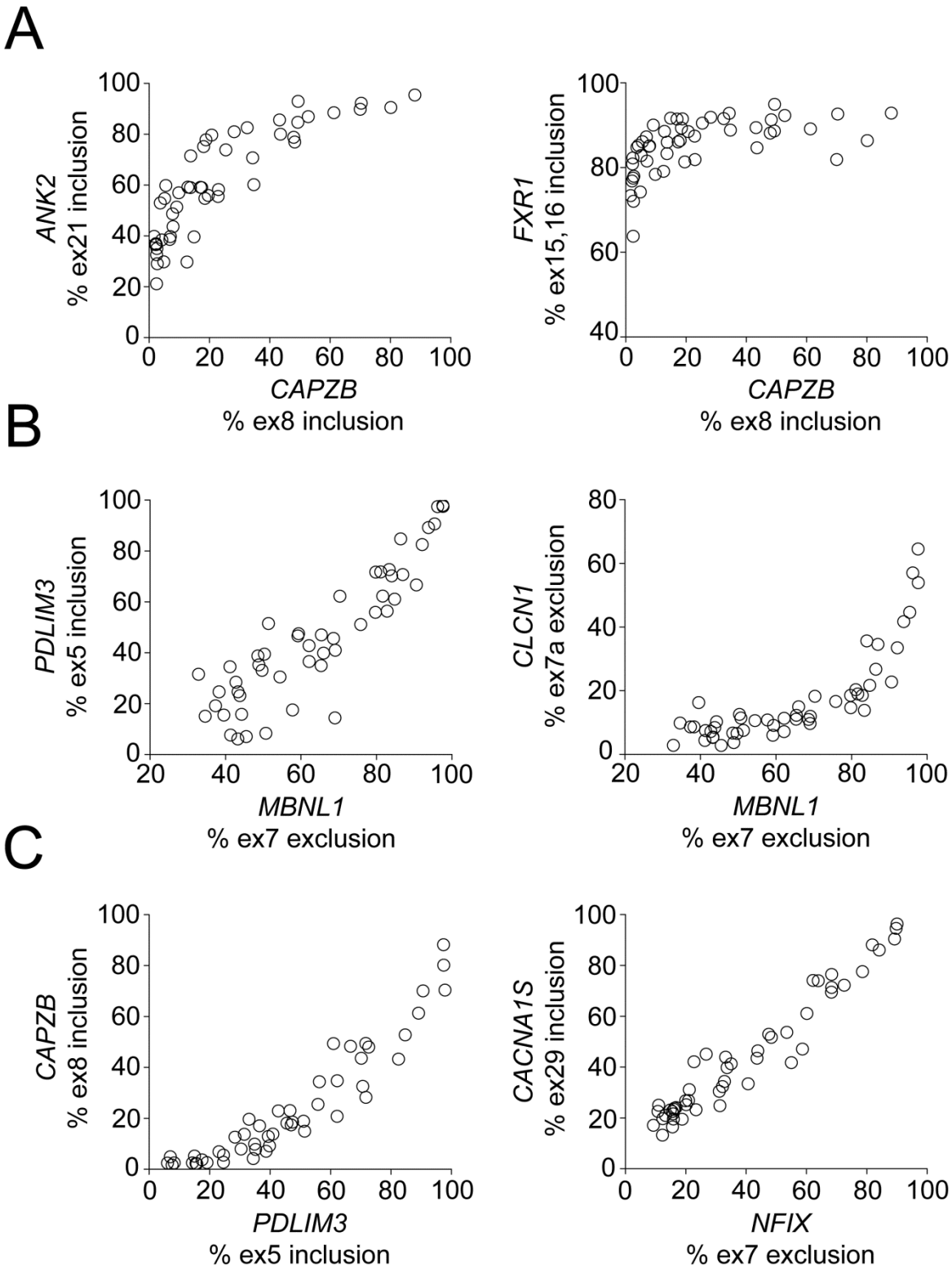

Supplementary Figure 9: Cross-correlation of splicing abnormalities in DM1. **(A)** *CAPZB* is more sensitive to DM1-induced mis-splicing than *ANK2* or *FXR1*. Some individuals with full DM1 mutations have strong skipping of *CAPZB* exon 8 (ex8) but normal or near-normal levels of *ANK2* exon 21 (ex21) or *FXR1* exon 15 and 16 (ex15,16) inclusion. **(B)** Cross-correlation of splice events that depend on MBNL1 but not CELF1. Whereas mis-splicing of *PDLIM3* and *MBNL1* are tightly associated (left panel), some individuals with mis-splicing of *CLCN1* (exon 7a exclusion below 60%) have normal or near-normal levels of *MBNL1* exon 7 inclusion (exon 7 inclusion above 80%, right panel) **(C)** Mis-splicing of certain exons is strongly associated (e.g., *CACNA1S* and *NFIX*, right panel) even when regulated by different splicing factors (e.g., *CAPZB* regulated by CELF1, and *PDLIM3* regulated by MBNL1, left panel).

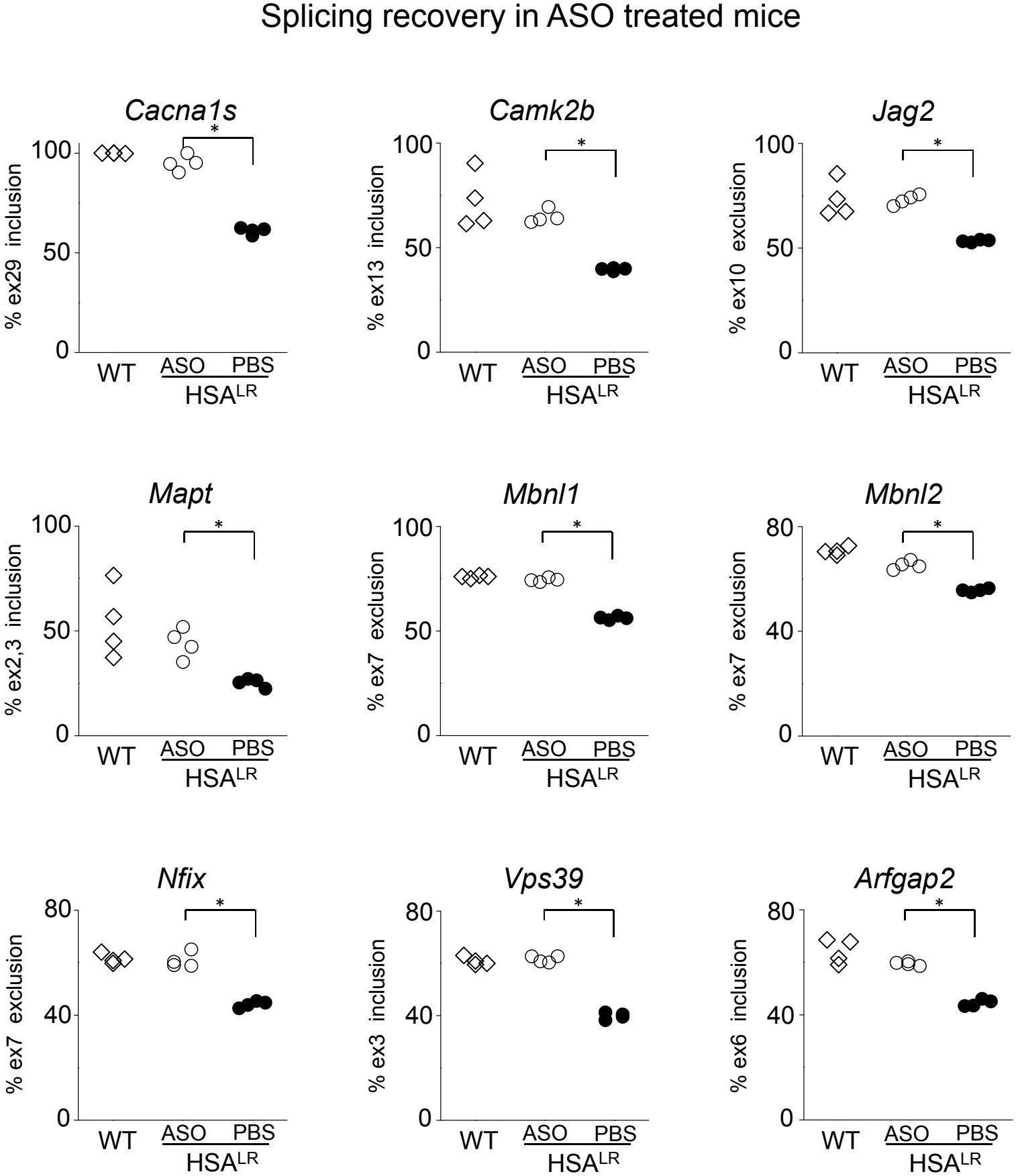

Supplementary Figure 10: Reversibility of DM-associated splicing defects in the HSA^{LR} transgenic mouse model of DM1. Nine splicing defects are fully reversed in HSA^{LR} mice by subcutaneous injection of antisense oligonucleotides (ASO) that target the transcript that carries an expanded CUG repeat. The ASO was administered by 8 subcutaneous injections over 4 weeks. Splicing was evaluated in quadriceps muscle.
* $P < 0.01$. PBS, phosphate buffered saline.